Experimental FEA . . . Much More Than Pretty Pictures!

George Fox Lang, Associate Editor

Until very recently, Finite Element Analysis (FEA) and Experimental Modal Analysis (EMA) have been very separate engineering activities aimed at solving a common problem. Now the two technologies are converging and powerful new tools for solving noise and vibration problems are emerging as a result. The recent term *Experimental FEA* has emerged. This article provides a "lab-rat's view" of what this term really means and why it is so valuable to today's S&V practitioner.

Experimental FEA is an integrated collection of modeling and analysis tools designed to be used by the *experimentalist*. It includes the facility to quickly build simple small-scale finite element models and solve them for natural frequencies and mode shapes. The intent here is not to replace the traditional analyst's tools, which are far more comprehensive and detail-focused. Rather, *Experimental FEA* is intended to augment the experimental understanding of structures by aiding us to perform better modal tests, faster.

Experimental FEA is essential to *test planning*. It provides scientific answers to questions that have long plagued our community, including:

- What *bandwidth(s)* must be used in the test of a new structure?
- *How many modes* must be identified within this bandwidth?
- Can I identify all of these modes from a *single reference* test, or must I collect *multiple-input multiple-output* (MIMO) measurements?
- *Where should I place my shaker* or shakers (or my reference accelerometers for a roving impact test) to achieve the best measurement results?
- *How many responses* (or impact sites) must I measure in order to draw clear and unambiguous animations of every mode?
- What is the *minimum number of frequency response functions* (FRFs) that must be measured to validate a large-scale FEM model of a new structure?
- *Where* should these responses be measured?

Past Meets Future

In the November 1989 issue of *Sound & Vibration*,[1] I reported results from applying Kistler's Translational/Angular Piezobeam™ (TAP) accelerometer to a free-free square plate. The experiment was conducted to evaluate the merit of measuring *rotational responses* as well as translational responses in a modal test. To properly evaluate the results, it was necessary to understand the mode shapes of the first few modes of free-free vibration. It was also important to understand the changes in these modes that the installation of the TAP sensor would impose. I called upon prior experiments conducted using *acoustic excitation and response measurement* to provide this. These non-contacting measurements made in approximated free-free condition were the best information then readily available to me.

Recently, I have had the opportunity to work with *Vibrant Technology's* **ME'scopeVES**. How I wish this Experimental FEA facility had been on my desk in 1989! A few minutes work provided me with the mode shapes shown in Figure 3. More importantly, I was able to rapidly model the effects of adding the 10 g TAP sensor to the plate's center.

This simple FEA was all that I needed to conduct my experiment with ease and confidence. Synthesized FRFs from this model would have provided ideal "sanity checks" for all of my experimental measurements, *including those made in rotational degrees-of-freedom* (DOFs).

As illustrated in Figure 4, formulating the plate model was a simple matter of choosing the type of substructure to model, applying the appropriate dimensions, orienting the plate in space and attaching quadrilateral FE plate elements to the drawing. These few entries created the geometric model and the *mathematical model*.

> *Experimental FEA is intended to augment the experimental understanding of structures by aiding us to perform better modal tests, faster.*

I chose *quadrilateral* elements for this thin plate. These have 24 DOFs – three translations and three rotations at each corner. Each quadrilateral is defined by its *thickness* and three *material properties*: density (δ), Young's modulus ($\mathbf{E}$) and Poisson's ratio (η). Library values for various materials are provided, or you can enter the properties for your material.

For a monolithic free-free structure, that's the whole entry process. Applying other boundary conditions or building a structure from multiple sub-structures requires a little more effort, most of it graphically guided.

An *eigensolution* (natural frequencies, damping and mode shapes) is accomplished at the push of a button. Even my aging 400 MHz Pentium II had little trouble in producing answers in acceptable time. This is one of the best characteristics of "desktop CAE" and small models; it encourages exploration of the model.

For example, Figure 5 illustrates that small models can be very effective at predicting modal properties. Here, the natural frequencies of the first five flexural modes of the square test plate are presented for different numbers (1 to 100) of quadrilateral elements used in the model. Note the rapid convergence of the answers. For practical purposes, a model with 36 quadrilateral elements will tell me as much (about these lowest modes) as one with 100 elements. Of course, it will do so in less computation time.

Other types of iterations, including material properties, can be profitable. While everyone knows that the natural frequencies of a plate are proportional to $\sqrt{\mathbf{E}/\delta}$, the effects of η are less commonly understood. *When one or more plate edges are free, the frequency of each mode is a function of Poisson's ratio*,[3] as illustrated in Figure 6. Available finite elements include *bars*, *rods*, *triangles*, *quadrilaterals*, *tetrahedrons*, *prisms* and *bricks*. The modeling library also contains simple elements including a *mass*, a *spring* and a *damper*. I used a mass element of 10 g attached to the plate's center to approximate the mounted TAP sensor. As anticipated, this only affected the 3rd (cupping) mode, as shown in Table 1.

How Many Shakers and Where?

Consider a hypothetical problem. You are required to test a physical bridge model that is basically a pin-ended beam. We have an FEA model of this structure (including estimated damping) as shown in Figure 7. Our assignment is to plan an EMA of this 2650 lb structure. Where do we excite it and how many shakers are required? (Or, how many fixed-location reference accelerometers are needed and where do we put them

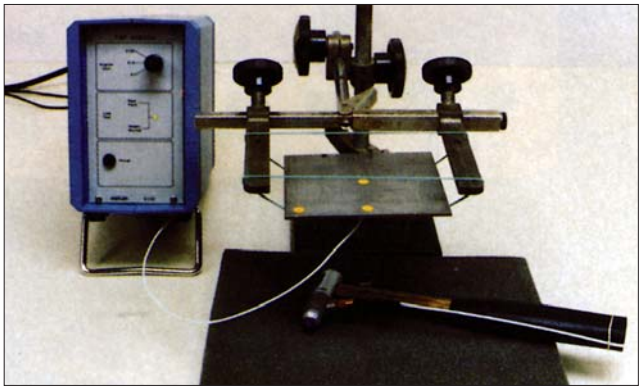

Figure1. 1989 impact test of free-free square plate and TAP sensor.

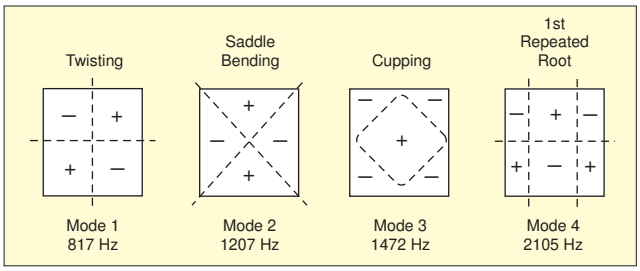

Figure 2. 1st four modes of the free-free plate measured acoustically (circa 1982).

for an effective roving impact test?)

We will start our test planning with the optimistic assumption that a *single reference* test will be adequate to identify all of the modes sought. In most cases, this assumption proves valid. The modal properties shown in Figure 6 reinforce this assumption, as *the model has no repeated roots*. All of the modes are unique in shape and frequency.

Hence, we will first search for an *optimum* DOF from which to excite (or observe) *all* of the modes of the structure. An extremely useful tool in this endeavor is the modal **Shape Product**[4] vector, defined by:

$$\{SP\} = \{\psi_1\} \cdot \{\psi_2\} \cdot \{\psi_3\} \ldots \{\psi_N\} = \prod_{n=1}^{N} \{\psi_n\} \qquad (1)$$

where $\{\psi_n\}$ is the n^{th} modal vector of the system.

This simple element-by-element product of the modal vectors can be displayed like any single mode shape of the structure. For plate-like structures, dominated by surface-normal motion, it is particularly useful to display the *absolute value* of the Shape Product as a *color contour*. Figure 8 illustrates such a display for the model bridge. At each DOF location, the Shape Product is the product of modal coefficients for *all modes* in a single DOF. If that DOF is a *node* for any one (or more) of the modes, the Shape Product is zero. The color contour is scaled from black (zero) to white (maximum) through the range of colors shown by the 'thermometer.' Thus, "bright spots" in the color contour locate DOFs where *all* of the modes *participate actively*. These locations are the best choices for a single shaker or reference accelerometer installation.

Four equally attractive reference locations (DOFs 36Z, 40Z, 136Z and 140Z) are marked by red arrows in Figure 8. Any one of these is appropriate for use in a *single reference* test and curve-fit.

The *real* and *imaginary* components of the driving-point

Table 1. Natural frequency (Hz) comparison.

	Acoustic Test	FE bare plate	FE 10 g added	TAP Test
Mode 1 – twisting	817	818.3	818.3	820
Mode 2 – saddle bend . . .	1207	1174	1174	1205
Mode 3 – cupping	1472	1455	1368	1340
1st repeated root	2105	2071	2071	N/A
1st repeated root	2105	2071	2071	N/A

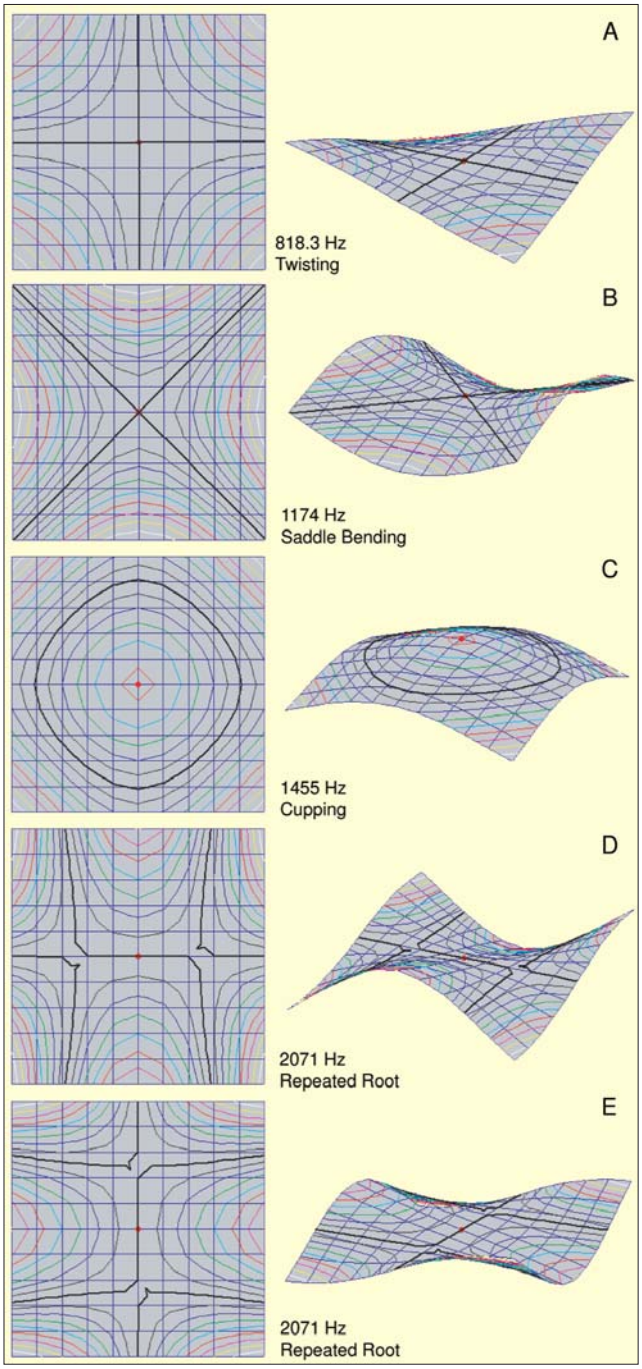

Figure 3. 2004 FEA of test plate.

FRFs for these four "hot spot" DOFs are overlaid in Figure 9. As intuition would suggest, these symmetrically arranged locations yield *identical* FRFs. Note, however, that the driving-point measurements of Figure 9 do *not* provide clear evidence of all six modes. *Five* clear peaks may be seen in the *imaginary* part. Each of these is bounded by a minimum and maximum in the *real* component.

Figure 10 expands the display of Figure 8 around the central peak. It is now clear that *two* peaks actually exist in the *imaginary* component, indicating the presence of two modes. However, it is also clear from the *real* component that the *half-power bandwidths* of these two modes overlap one another.

From Figure 7 we note the 3rd mode is of twisting or *torsional* character and occurs at 22.84 Hz with 1.764% damping. The 4th mode is a *bending* shape at 23.46 Hz with 1.791% damping. These modes are clearly *distinct* as opposed to *repeated* roots. However, they are *closely-coupled* or *overlapping* modes that are difficult to identify from a *single reference* test. These modes are closely-spaced in frequency solely because of the

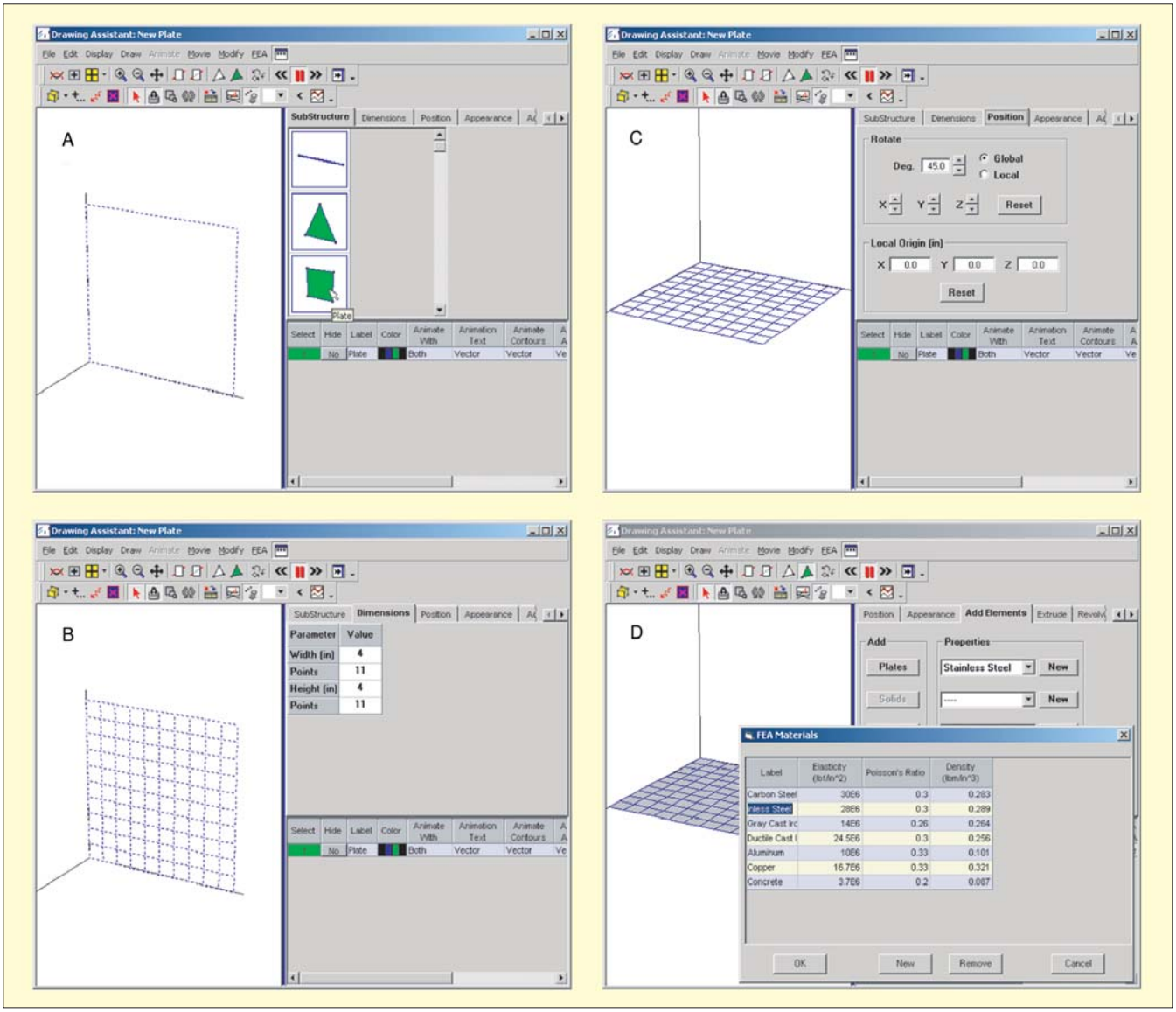

Figure 4. Steps in building FEA: A – select type of structure, B – add dimensions, C – orient the model, D – add finite elements.

length/width/thickness ratios of the model bridge (and its boundary conditions). The two modes in question have light damping.

An earlier work[2] provided a definition for the oft-bandied term *modal density* (MD) and comments upon its impact on modal curve-fitting. The 3rd and 4th modes of this model have an extremely high local modal density of 0.6638 between them, defined by the natural frequencies and damping factors of the two modes in accordance with:

$$\mathrm{MD}_{3,4} = \frac{(\xi_3 f_3 + \xi_4 f_4)}{2*(f_4 - f_3)} = \frac{(1.764*22.84)+(1.791*23.46)}{200*(23.46-22.84)} = 0.6638 \quad (2)$$

Note that improving the frequency resolution of the FRF measurements will *not* enhance the separation of these two modes. The precision of modal parameter identification is limited by *frequency resolution* for modal densities of 0.2 and less. For modal densities between 0.2 and 1.0, the limiting factor is the *sophistication of the curve-fitting algorithm*. When the modal density exceeds 1.0, the limiting factor is the ability to determine *the number of modes* in the frequency bandwidth.

Because the half-power bandwidths of the 3rd and 4th modes overlap significantly, these modes *must* be identified using a curve-fitter that can detect *multiple modes* within a single "fit interval." SDOF fitters *will not work effectively* at this modal density level.

Figure 11 illustrates a highly automated "Quick Fit" to the driving-point FRF at DOF 40Z. It successfully identified all six modes precisely because this FRF 'disclosed' two modes near the central peak to the *modal peaks indicator* function and the companion MDOF fitter could extract their properties.

Figure 12 illustrates the same algorithm applied to all possible driving-point FRFs *except* those at DOFs 36Z, 40Z 136Z and 140Z. That is, all possible driving-point FRFs except those identified by the Shape Product as optimum references are fitted. Note that only *five* modes are identified. The 4th mode at 23.46 Hz was 'missed' by this curve-fit to 171 FRFs.

If the actual structural model deviates even slightly from the FEA model, it may not be possible to gain an accurate mode count from the experimental measurements at any DOF.

The explanation for this "five-mode finding" is simple. None of the 171 "non-optimum" DOFs gave evidence of the 4th mode to the *modal peaks indicator* function. Five modal peaks were found in the 171 FRFs and five modes were fitted to the data. This can be better appreciated by viewing Figure 13 which overlays the *imaginary* components of the driving-point FRF at 40Z (red trace) with those of the four "next best" DOFs (55Z,

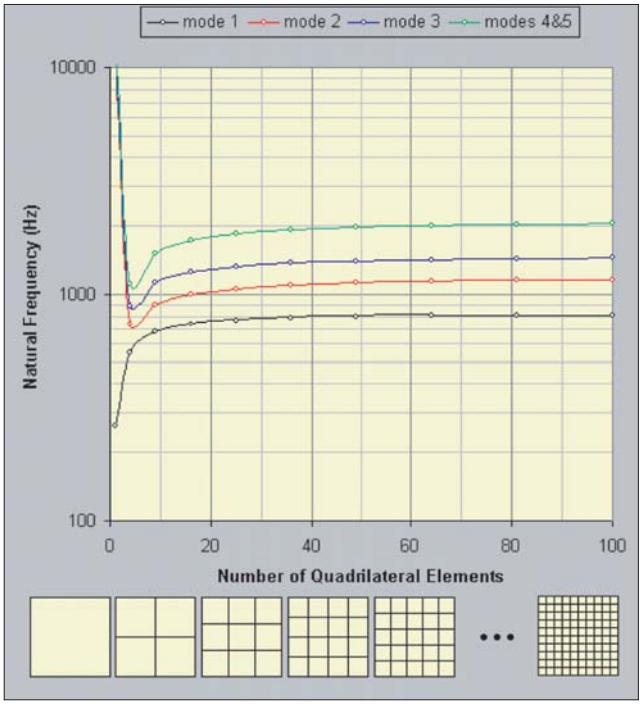

Figure 5. Convergence of natural frequencies with increasing number of quadrilateral elements.

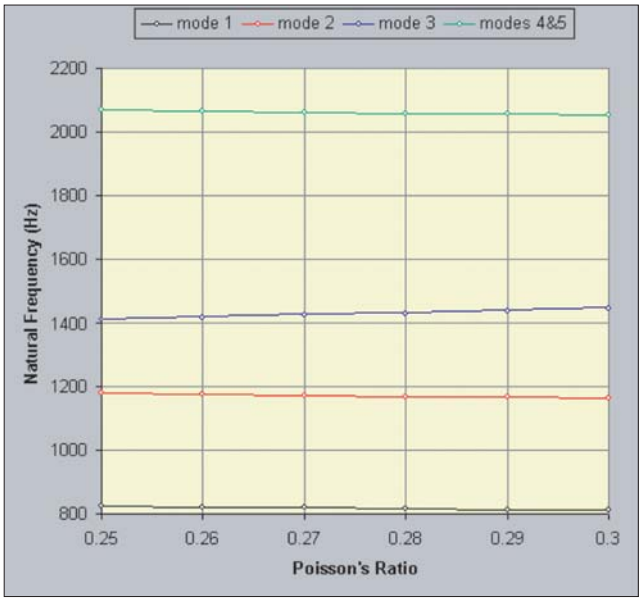

Figure 6. Effect of Poisson's ratio on free-free square plate natural frequencies.

60Z, 70Z and 75Z) identified by the Shape Product of Figure 8.

Figure 14 expands the comparison plot of Figure 13 around the central peak. Observe that only the red "first choice" reference (40Z) gives any graphic hint of the 4th mode at 23.46 Hz. While 4th mode participation is there, it is at too low a level to allow the *number of modes* to be properly counted. Hence, the Shape Product "hot spots" accurately identified the *only* four DOFs from which all modes could be identified by a *single reference* test. While a *single reference* test is *possible*, it would be an imprudent choice for this structure.

If the actual structural model deviates *even slightly* from the FEA model, *it may not be possible to gain an accurate mode count* from the experimental measurements at *any* DOF. A slight increase in the 3rd modal frequency, a reduction in the 4th modal frequency or an increase in damping factor for either or both modes could increase the local modal density sufficiently to obscure one of the closely-coupled modes from

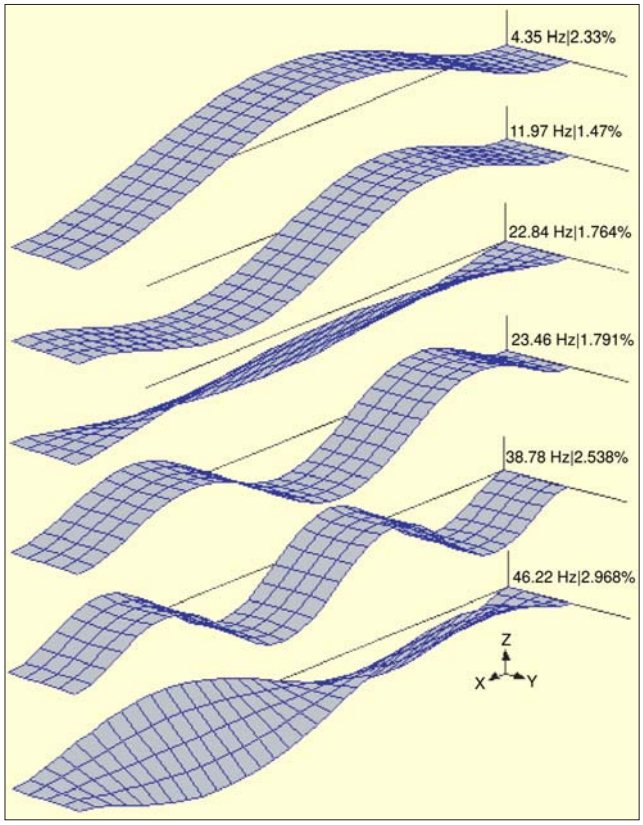

Figure 7. First six modes of a pin-pin beam.

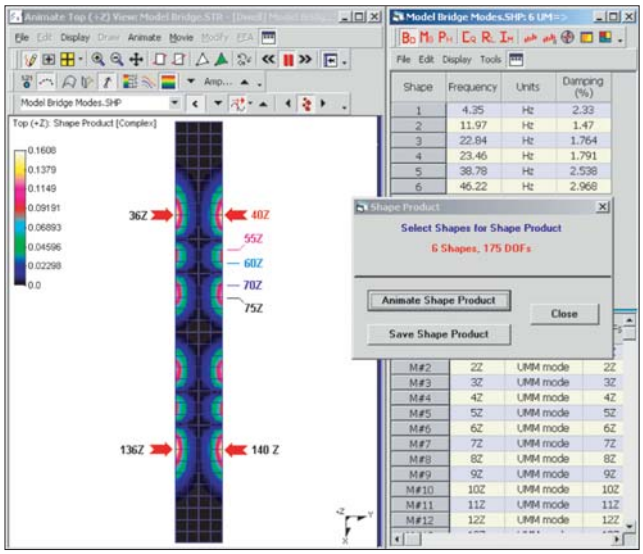

Figure 8. Shape product of beam modes.

detection *anywhere* on the structure.

Hence, the model bridge is a proper candidate for MIMO measurement and *multiple reference* curve-fitting. *At least two* shakers or fixed-position reference accelerometers are required to test this structure effectively.

Selecting Multiple Reference Sites

Attempting to find an optimum site for a single shaker (or reference accelerometer) disclosed that *at least two* reference DOFs are required to physically separate the frequency-proximate 3rd and 4th modes. The specific problem to be solved is the *spatial separation* of these two modes.

Since the 4th mode at 23.46 Hz was obscured by the 3rd mode in all measurements examined so far, we will start our test design by choosing a DOF from which the 4th mode can be readily excited. Figure 15 provides insight regarding this matter.

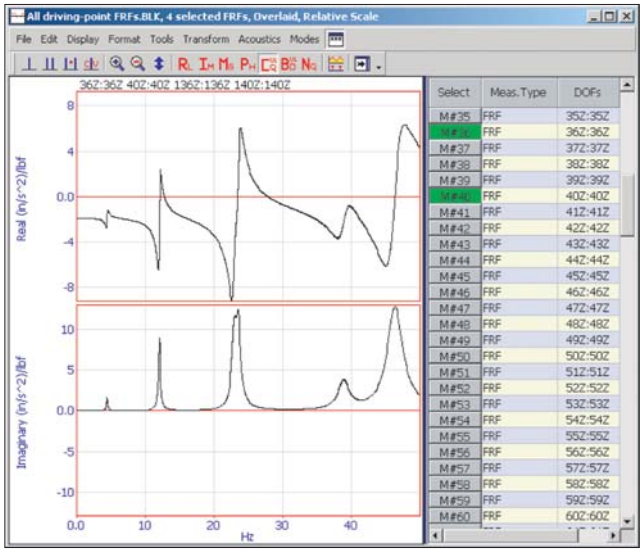

Figure 9. Overlay of driving-point FRFs at four shape product "hot spots."

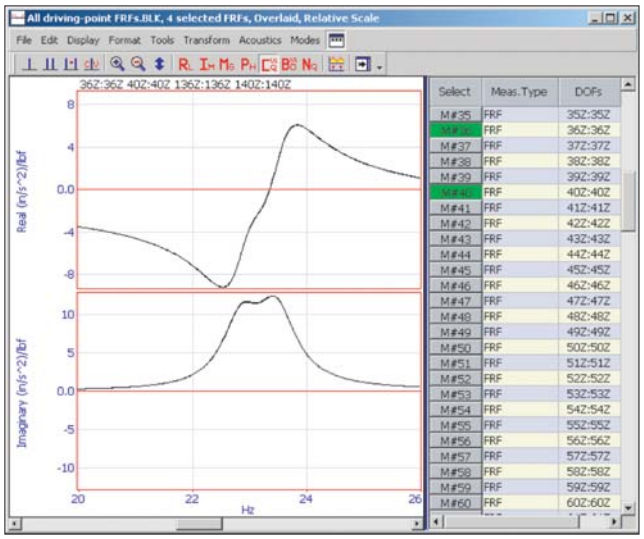

Figure 10. Zoom around 3rd and 4th modes.

Figure 15 repeats the six mode shapes shown in Figure 7 in a different format. The modes are shown as color contours, presenting the *absolute value* of response shape. Note that mode 4 can be readily excited from bridge-centered DOF 88Z, which will also provide strong excitation of the 1st mode. It will not excite modes 2, 3, 5 or 6 as it lies on *nodes* for all of them. Hence a shaker at 88Z will excite *only* the 1st and 4th modes.

We now need another DOF from which to excite the remaining 2nd, 3rd, 5th and 6th modes. The Shape Product gives us a means of identifying this location. Figure 16 illustrates the Shape Product for modes 2, 3, 5 and 6 *only*. Note that four symmetrically oriented "hot spots" including DOF 65Z are indicated. Hence, a reference at 88Z will drive (or respond to) modes 1 and 4. A second reference at 65Z will interact strongly with modes 2, 3, 5 and 6, but not with mode 4.

Most importantly, these two references provide *spatial* or *physical* separation between modes 3 and 4 as shown by Figure 17. Note that DOF 88Z, which can excite the 4th mode readily, is at a *node* for the 3rd mode, so that it will not exchange energy with it. In contrast, DOF 65Z can interact readily with the 3rd mode, but is at a *node* of the 4th mode.

Figure 18 illustrates the benefit of this spatial separation. The *imaginary* component of three driving-point FRFs are compared here. The red trace is the 40Z FRF previously selected for a *single reference* test. This is followed by the driving point FRFs at 65Z and 88Z, the optimum sites for a *dual reference* MIMO test.

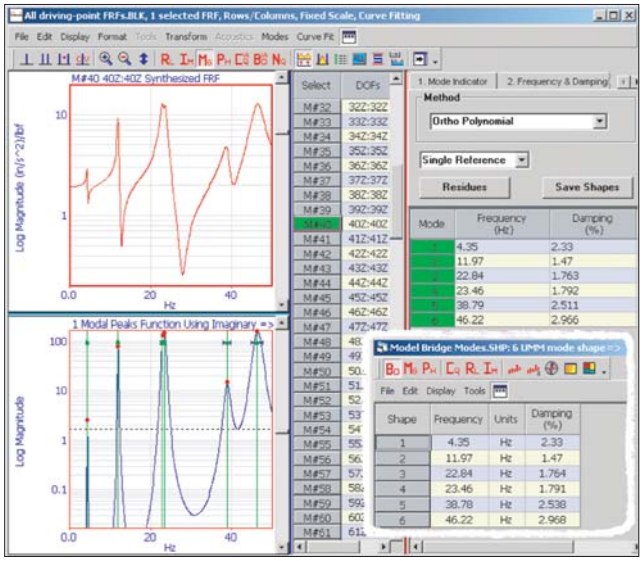

Figure 11. Curve-fit of one "hot spot" driving-point FRF identifies all six modes.

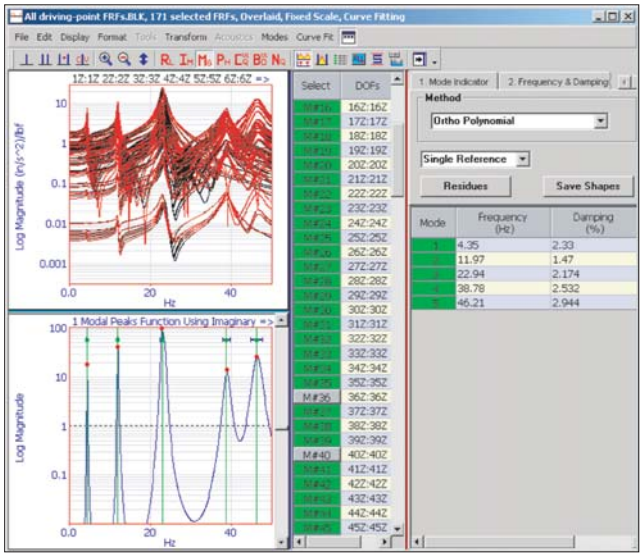

Figure 12. Curve fit of remaining 171 driving-point FRFs fails to identify the 4th mode.

Note that the dual reference test will excite all of the modes, but will do so *selectively*. The 88Z reference will drive (or respond to) only the 1st and 4th modes. The 65Z reference will drive (or respond to) only the 1st, 2nd, 3rd, 5th and 6th modes.

Observe that the 2nd, 5th and 6th modes can receive essentially *equal* excitation from either the *single reference* or *dual reference* tests. The *dual reference* test will provide *more* excitation to the 1st mode as well as separated and increased excitation of the closely-coupled 3rd and 4th modes.

Figure 19 illustrates the results of applying an automated *multiple reference* curve-fitter to the driving-point FRFs for DOFs 65Z and 88Z. Note that all six modes are precisely identified.

Hence, our model bridge can be well measured by applying shakers (or reference accelerometers) to DOFs 65Z and 88Z. The data can be reduced by applying a *multiple reference* curve-fitter using *two* references.

How Many Responses for Pretty Pictures?

It is normally considered good practice to use sufficient test DOFs to characterize each Mode Shape with reasonable fidelity for human viewing. *Reasonable fidelity* is commonly accepted to be about 10 points/cycle along any axis with sine-like deformation.

Inspection of Figure 7 discloses that sine-like deformation

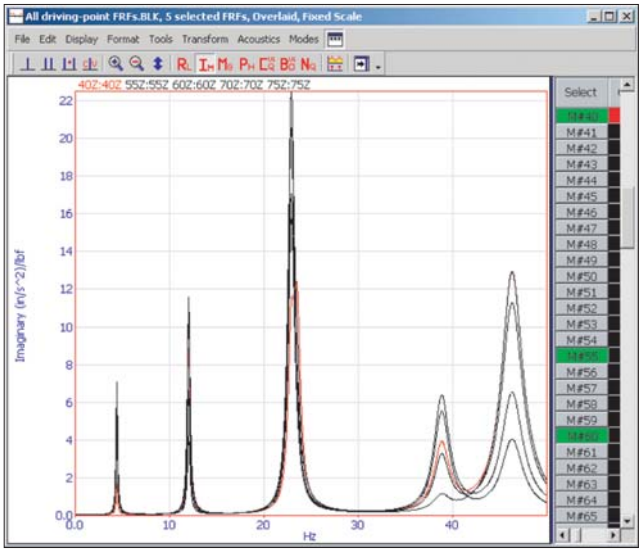

Figure 13. Driving-point FRF comparison of one "hot spot" (red) with four "second best" locations.

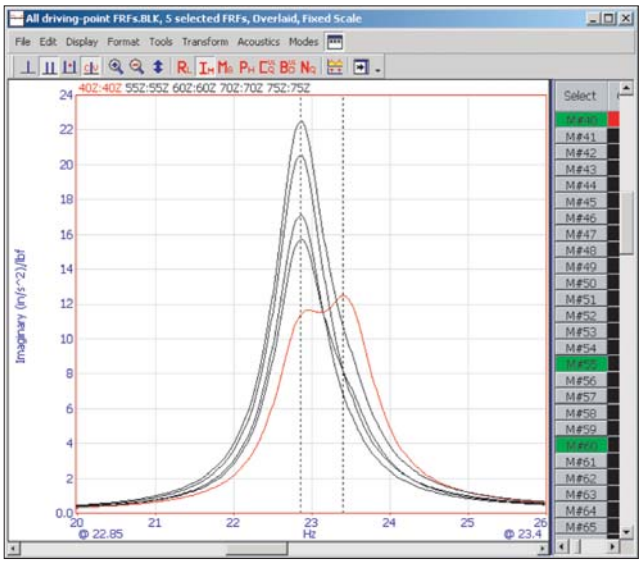

Figure 14. Zoom of comparison around 3rd and 4th modes.

occurs along the X-axis of the bridge. The highest "spatial frequency" is two sine cycles along the span. This occurs in the 38.78 Hz 5th mode. Hence we want about 20 equally-spaced points in the X-direction. Along the Y-axis, the deformations appear to be straight lines. Three equally-spaced points along the Y-direction will be sufficient to verify this shape.

As shown in Figure 20, selecting every other point from our (small) FEA mesh will result in a grid with 19 points along the X-axis and 3 along the Y-axis. This agrees well with our *reasonable* fidelity guidelines. Of these 57 points, 6 are *fixed boundary points that do not move* for which measurements will *not* be required. Since our FEA mode shapes only contained Z-direction DOFs, our test model is reduced to 51 DOFs where responses must be measured.

However, our 'decimated' model *must* contain DOFs 65Z and 88Z as these are the intended references to which shakers will be applied. Since point 65 does not fall on our alternate-point grid, we must add 65Z as the 52nd DOF and our model will contain 58 geometric points.

We will prove the adequacy of the spatial sampling provided by the 58 point, 52 DOF model by comparing it with the original 175 DOF FEA and with a smaller, inadequately sampled, model. Figure 21 illustrates a 27 point model including 21 DOFs. This model only provides 9 points along the X-axis, less than half of those required by our *reasonable fidelity* rule-of-thumb. Since the DOFs included in both of these small models are subsets of the original FEA model's DOFs, we can animate the FEA modes using either model.

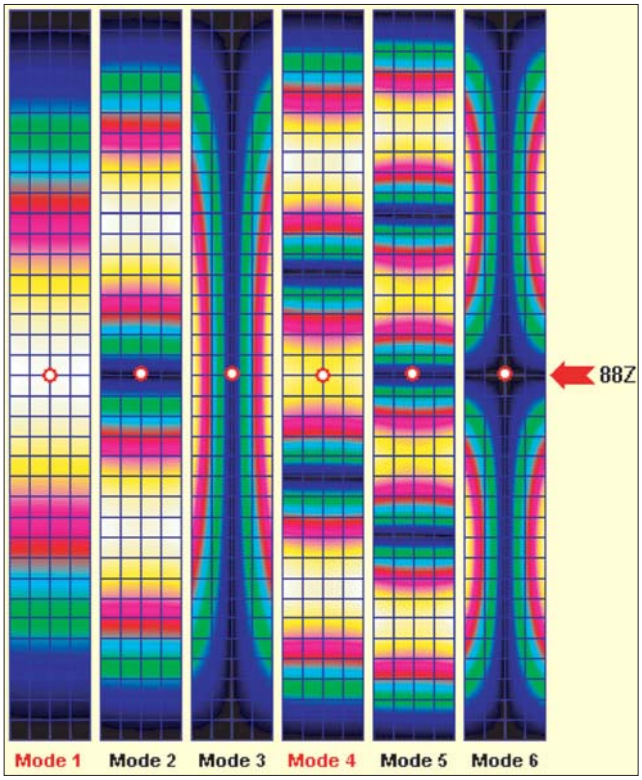

Figure 15. Selecting a reference site to drive mode 4.

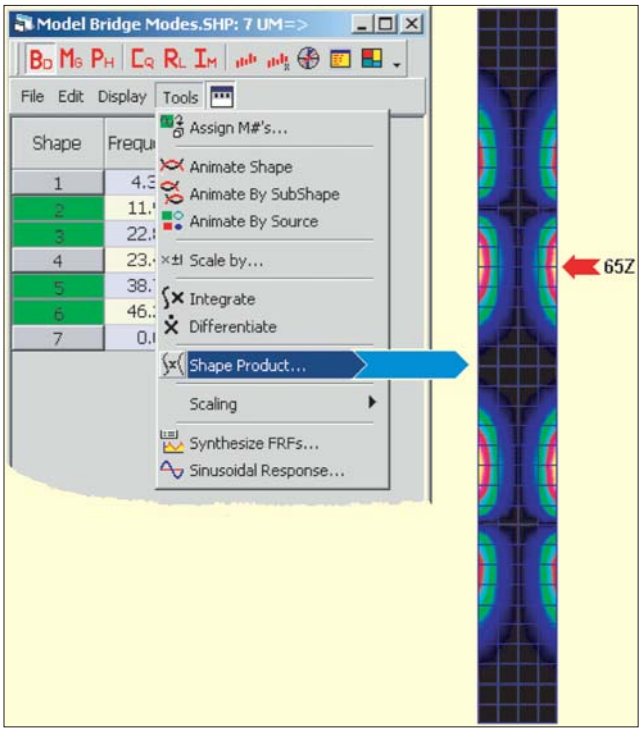

Figure 16. Selecting a site to excite modes 2, 3, 4 and 6.

As illustrated by Figure 22, displaying the mode shapes using the 58-point model conveys all of the information provided by the original 175 DOF FEA model (Figure 7). Animation using the 27-point model of the structure results in some confusion about the shape details, particularly for modes 4 and 5. This validates the "10 point-per-cycle" *reasonable fidelity* rule-of-thumb.

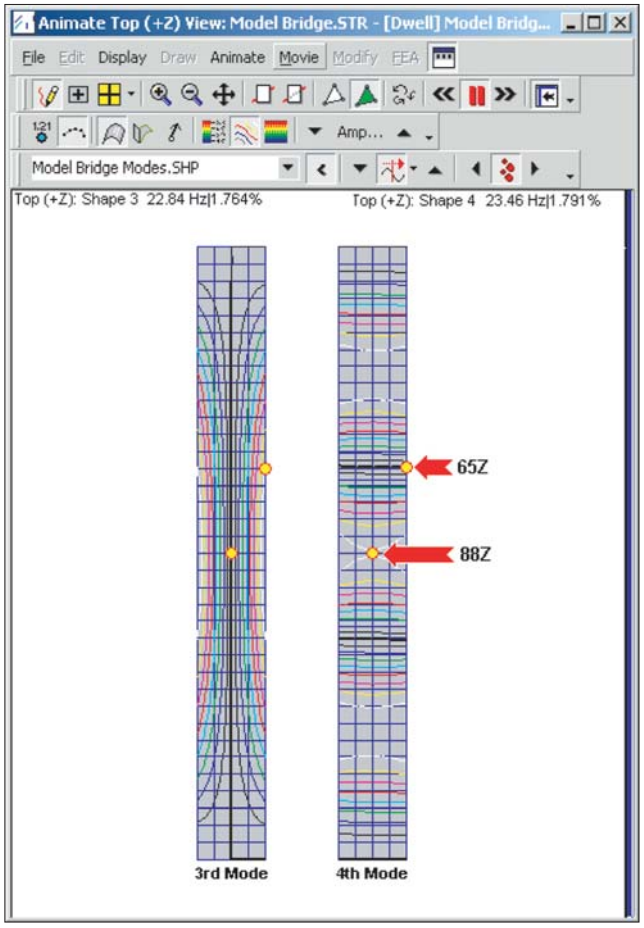

Figure 17. Selected reference sites optimize physical separation of frequency-proximate modes 3 and 4.

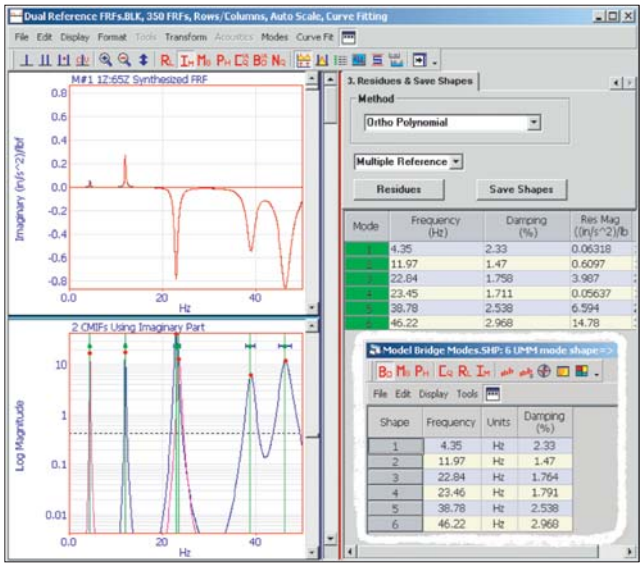

Figure 19.Verification curve-fit of dual-reference measurements identifies all six modes.

Baring the Minimum

Clearly, the 52 DOFs of the 58 point model are adequate to describe the six modes. However, we are often required to simply *test validate* an FEA *using the smallest test possible*. We need a scientific means of selecting a very small sub-set of the FEA mode shape DOFs that will accurately represent the *shapes*. The *Modal Assurance Criterion* (MAC) provides a tool to accomplish this.

In particular, we will use the *Auto MAC* to compare each FEA mode shape with *itself* and *all other modes in the model*. Figure 23 illustrates the Auto MAC of the FEA modes.

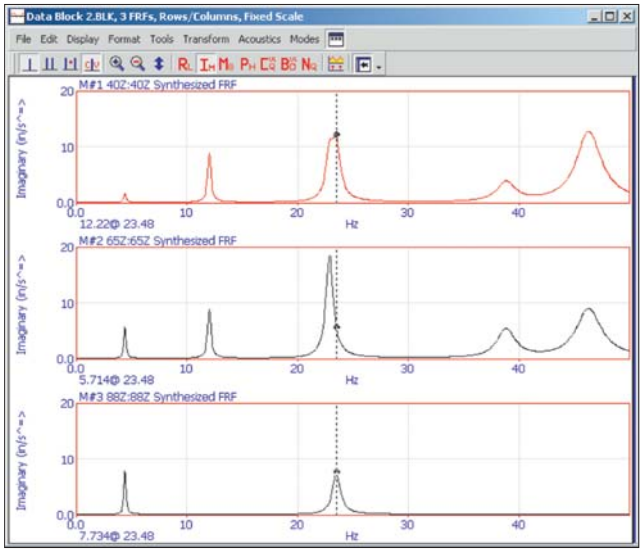

Figure 18. Comparison of driving-point FRFs for single (red) and dual-reference test designs.

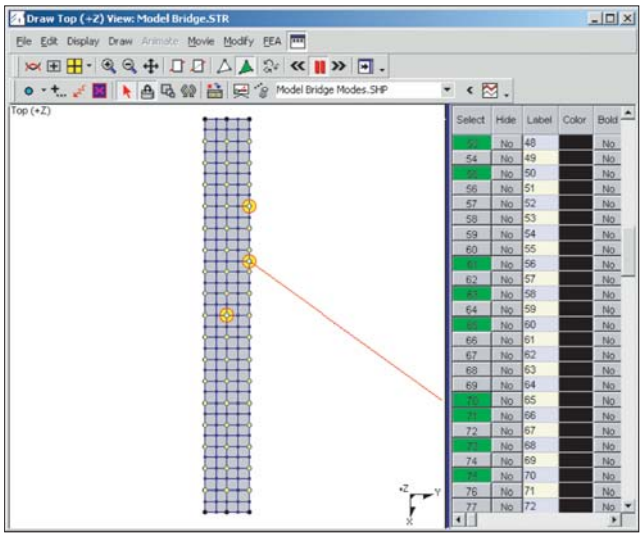

Figure 20. 58 point "reasonable fidelity" model.

Note that the MAC matrix is a 6-by-6 *identity matrix* with 1s on the diagonal (orange highlight) and 0s in all of the off-diagonal locations. These MAC coefficients compare the *shapes* in the model with one another. Each row and each column represent one Mode Shape and the coefficient at each intersection expresses the similarity of a row and column mode. A value of 1 indicates a perfect match, 0 indicates no similarity. A value of 0.9 or greater indicates strong similarity between the two shapes.

Since we are comparing the six modes of an FEA, we know the MAC must be a perfect identity matrix. Each of the mode shapes is *linearly independent* of all the others, as the shapes are known to be *orthogonal* with respect to the model's mass matrix.

The MAC matrix can be plotted as shown in Figure 24. When the Auto MAC is a perfect identity matrix, the plot shows only unit height bars down the diagonal of the display. The preceding MAC figures used all 175 DOFs of the FEA mode shapes. We will now investigate using a much smaller number of DOFs in the Auto Mac computation.

When the Auto MAC is calculated using only *one* DOF, the resulting MAC matrix has 1s in *every* location, as illustrated by Figure 25. In this instance, DOF 40Z (a *single reference* "hot spot") was used. However, it does not matter *which* single DOF you select, the result is always a matrix with 1 as the value of every element. This result makes it clear that while a single FRF *may* be adequate to identify the *natural frequencies* and *damp-*

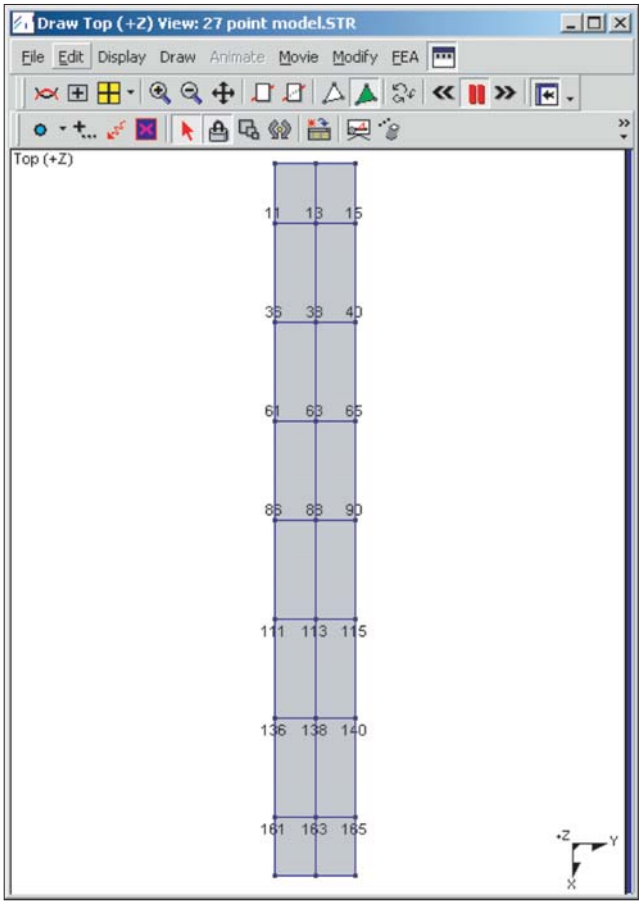

Figure 21. 27 point, 21 DOF structural model.

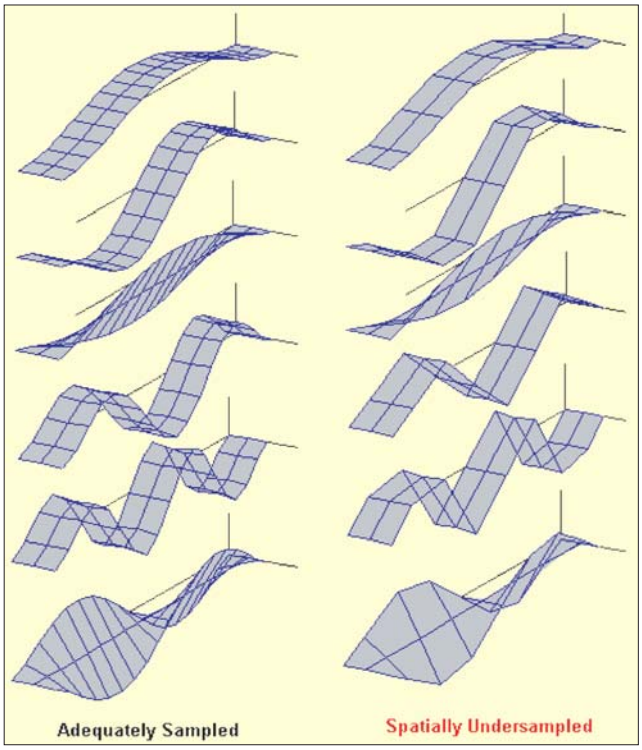

Figure 22. Comparison of FEA mode shapes using 58 point (left) and 27 point (right) structure models.

ing factors of the structure, it provides no insight regarding the mode *shapes*.

We would like to build a test model that can serve to validate the FEA using *multiple reference* testing, with DOFs 65Z and 88Z as the references. Therefore, we will repeat the MAC calculation adding these degrees-of-freedom. The resulting 3

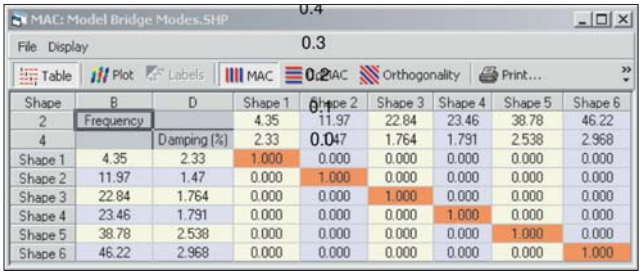

Figure 23: MAC matrix using 175 DOF FEA model.

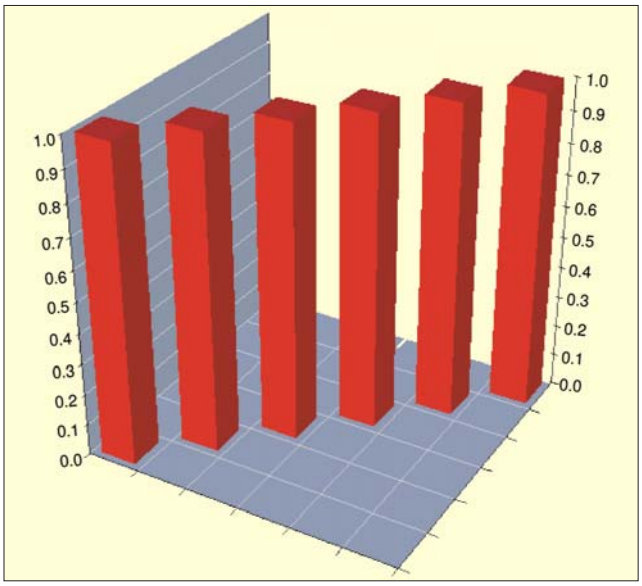

Figure 24. Plot of MAC matrix for all 175 DOFs.

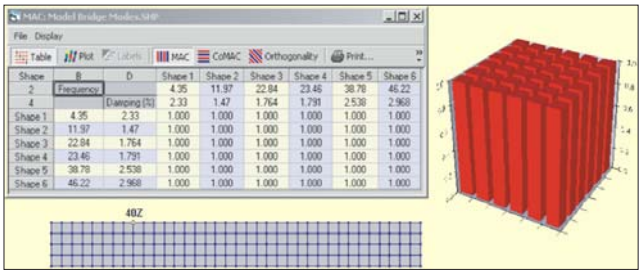

Figure 25. MAC for DOF 40Z only.

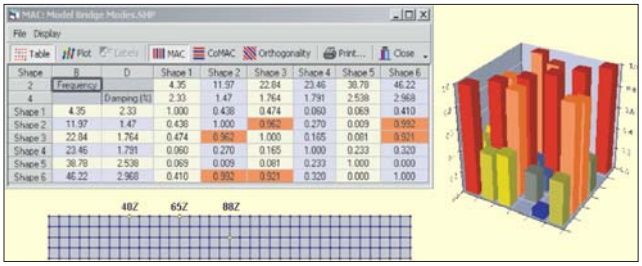

Figure 26. MAC for reference DOFs 40Z, 65Z and 88Z only.

DOF MAC is shown in Figure 26. With these three DOFs selected, the MAC matrix has far fewer significant elements. All of the diagonal elements have a value of 1. However, six off-diagonal elements (highlighted in orange) still have values greater than 0.9, indicating that this set of three DOFs cannot discriminate between mode shapes 2, 3 and 6.

We need to add additional DOFs to improve the shape selectivity. As a criterion for success, we will demand that all *off-diagonal* MAC *elements have a value of 0.1 or less*. The objective is to add as few DOFs as possible to achieve this goal. One satisfactory solution is the addition of DOFs 36Z, 61Z, 111Z, 115Z and 140Z as illustrated by Figure 27.

Note that our criterion is solidly met. The worst-case off-

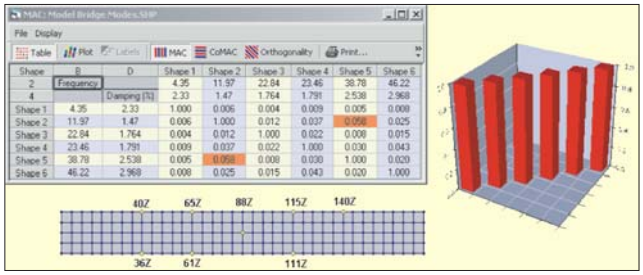

Figure 27. MAC using eight DOFs including the references.

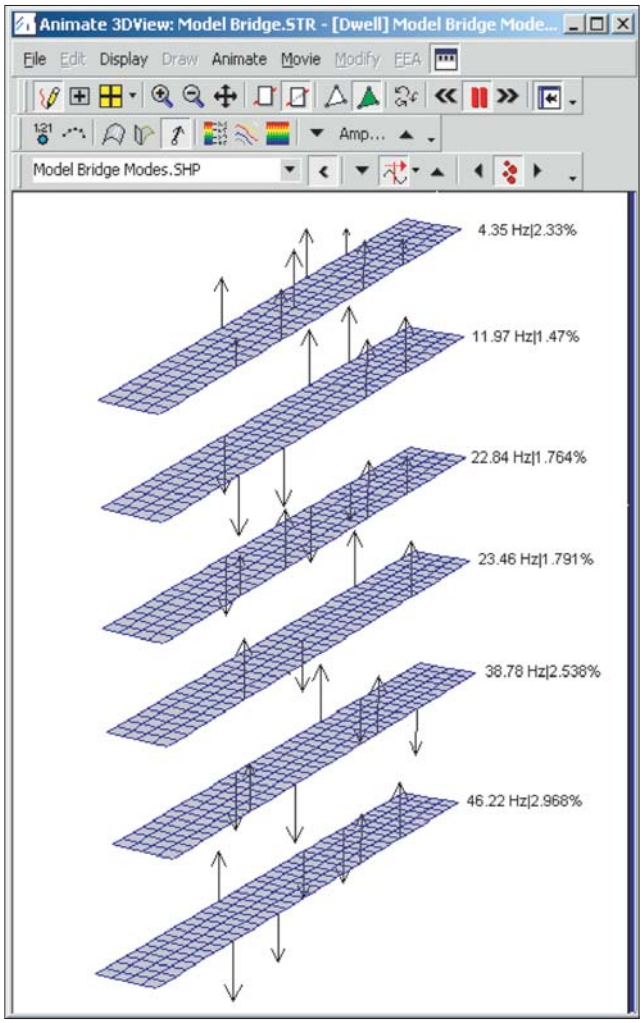

Figure 28. Mode shapes represented by eight DOFs.

diagonal elements have a value of 0.058. This MAC solution indicates that *these eight DOFs are sufficient to validate the FEA model's six mode shapes*. Either a *single reference* test measuring 8 FRFs referenced to a force at 40Z or a (two-shaker) *multiple reference* test measuring 16 FRFs against 65Z and 88Z force inputs may be employed. The 'correctness' of each *test measured* mode shape may then be evaluated by calculating a *Cross MAC* between the measured and FEA mode shapes.

> *Experimental FEA . . . is clearly the most valuable modal test-planning tool ever placed at our disposal.*

Thus, iteratively calculating Auto MAC matrices using only *selected* DOFs from the FEA modes allowed us to determine that *this FEM can be test validated by measuring only eight responses*.

However, such a 'minimized' test will not provide *reasonable fidelity* for human viewing as illustrated by Figure 28. Eight DOFs are simply insufficient to capture the distinct graphic nature of each mode shape. But this small data base *is sufficient* to mathematically determine if the physical test object exhibits the same modal properties as the FEA which models it.

Conclusions

The tight integration of FEA with testing software clearly permits a modal test to be designed scientifically. Eliminating trial-and-error experiments from the EMA setup phase saves time and produces better testing results.

Experimental FEA will doubtless provide other benefits to the experimentalist and the analyst as time ensues and experience increases. But, should it never solve another problem, it is clearly the most valuable modal test-planning tool ever placed at our disposal.

References

1. Lang, G. F. "Including Rotational Terms in a Modal Model . . . An Experimental Prelude." *Sound & Vibration*. November 1989.
2. Lang, G. F. "Modal Density – a Limiting Factor in Analysis." *Sound & Vibration*, March 1983.
3. Leissa, A. W. "Vibration of Plates." NASA SP-160. National Aeronautics and Space Administration, Washington DC. 1969.
4. Schwarz, B., Richardson, M., Avitabile, P. "Locating Optimal References for Modal Testing." IMAC 20, January 2002 (available at www.vibetech.com).
5. "Choosing Reference DOFs for a Modal Test." Application Note #24. Vibrant Technology, Inc. Scotts Valley, CA, 2004 (available at www.vibetech.com).
6. "Choosing Response DOFs for a Modal Test." Application Note #25. Vibrant Technology, Inc. Scotts Valley, CA, 2004 (available at www.vibetech.com).

The author can be contacted at: george@foxlang.com.